Anomalous behavior of the MRI during EPOXI approach to 103P/Hartley 2

Dennis Bodewits, Don Hampton, Ken Klaasen, Steve Wissler, Tony Farnham,
and the DIXI team.

Summary: We conducted three diagnostic tests to try to isolate the cause of the 'CN anomaly' detected during the approach to comet Hartley 2. The first test involved imaging with the LED STIM lamp turned on, the second involved imaging while the MRI pre-amp temperature set points were adjusted, and the third conducted imaging with the spacecraft attitude modified to provide the same Sun illumination geometry as during the anomaly to check for light leaks. We found that LED flickering would result in a clear pattern on the MRI CCD, which was not observed. Thermal variations might introduce noise, and it is likely that sudden variations in the electronics can be responsible for part of the anomaly. However, the light leak test best reproduced the signal levels and morphology observed in both filters during the CN anomaly. We conclude that the anomaly was caused by a small light leak that allowed some sunlight to enter the instrument for solar elongations between 118° and 128°.

1. Introduction

A significant anomaly in the MRI background level was encountered during the approach to Hartley 2. From 60 days before encounter (E-60d) to E-40d, MRI images of Hartley 2 were obtained through the clear and the CN (387 nm) filters. Between E-56d and E-42d, the observed signal level in the CN filter gradually increased tenfold above normal from 0.002 DN/s/pixel to 0.02 DN/s/pixel and then decreased to its original level again. The clear-filter images showed a 50% increase peaking from 0.04 to 0.06 DN/s/pixel – i.e., an absolute increase of approximately 0.02 DN/s/pixel in both filters. The CN exposure times were 480s compared to the clear exposures of 60s. The enhanced signal was nearly uniform across the entire frame (>150,000 km from the nucleus) at every time step, which cannot be explained by any plausible natural phenomenon related to the comet as any comet-related cause would exhibit spatial development with respect to the nucleus.

These observations led us to suspect that the signal increase was due to some instrumental effect. Three hypotheses for the cause of the "CN anomaly" were offered: 1) a change in CCD dark signal or readout offset or gain due to changes in electronics temperature, 2) stray light reaching the detector from some source behind the filter wheel, and 3) low level LED glow due to magnetic induction. A set of image sequences was designed to obtain data to test each of these possibilities. The test sequences and their results are described below. For all the tests, calibrated images (RADREV) from the UMD SDC were used to perform the analyses.

2.1 LED light

The CCD channels include an in-flight LED stimulator mounted within the light blocker structure that can shine onto the back of the light blocker blade when it is

held closed. Stimulator images are used to detect changes in the CCD performance. It was thought that the LED might have had a faint glow, induced by an unknown source (possibly magnetic induction or scintillation by cosmic rays), and the resulting light was reflecting off the backside of the filters to produce the anomaly. Observations to test for this case were obtained on DOYs 2011285 – 2011286. Using both MRI and HRI, we measured the strength and color in the LED signal reflected off of the filters, and searched for a fixed pattern. While this scenario was pretty far-fetched, it was the easiest test to conduct, and would give us some information on the LED spectral characteristics and illumination. Since we did not know what flux to expect, we used 4 different exposure times of 60, 600, 6,000, and 60,000 msec, using the full frame (1024 x 1024) with both the CN and the CLEAR1 filters. The shutter was held open during this test.

We used the 600 msec exposures for both the MRI and HRI images, as these images had excellent SNR without suffering from saturation effects (longer exposures) or contamination by background stars (shorter exposures). Quadrant label assignments follow Klaasen et al. (2008) and are shown in Figure 1.

The LED reflection results in a clearly distinguishable pattern on the chips (Figure 2). For the MRI, this pattern consists of a slightly curved intensity gradient, resulting in a 30% difference between the two quadrants on the left (B & D) and on the right (A & C) of the detector. For the HRI, this pattern appears more complex, with the maximum brightness in quadrant A and a curved gradient from right to left (10% difference between left and right; there is a 3% difference between A & C). Maximum count rates with the LED fully on were 13.3 DN/msec/pixel (MRI CLEAR1) and 27.2 DN/msec/pixel (HRI IR).

For each of the images we determined the total counts per quadrant, avoiding a 10-pixel area close to the edges. The resulting total counts for MRI and HRI are summarized in Figure 3. The data are organized by wavelength rather than by time of acquisition; comparison between the first and last image, both obtained using CLEAR1, shows a ~2% variation (MRI) over the course of the LED test. While the reflectivity of the back surface of the filters varies a lot, we find an average (whole chip) count ratio CN/CLEAR1 between 0.99 – 1.02 (compared to CN/CLEAR1 ~ 0.3 during the anomaly). This probably implies that most of the light reaching the detector was reflected not by the filters but by other surfaces on the inside of the camera. In the HRI data, there was no variation in time between the counts measured in the different CLEAR1 and CLEAR6 filters, and no clear trend with color.

2.2 Preamp temperature variations

The second potential cause of the anomaly involved changes in the electronics temperature that could have altered the CCD dark signal, readout offset or gain, introducing additional signal not reflected in the overscan pixels. Between DOY 2010248 and 2010268, the HRI was powered off and then back on due to elevated temperatures in some spacecraft telecomm components. Several MRI electronics temperatures shifted by about 7°C from their usual values (three measured colder, one measured warmer) and then back again in conjunction with the HRI power cycles and roughly correlated with the CN anomaly period. Preamp temperatures returned to their normal values one to two days before the anomaly ended. The

temperature of the electronics boxes inside the spacecraft decreased by approximately the same amount during this period, suggesting that there might be a correlation between the temperature and the elevated background. While it is difficult to remotely change the electronics box temperatures, it is simple to change the preamp temperatures. We therefore gradually increased the temperature of the MRI preamp box to test if temperature changes could induce variations in the CCD dark signal, the readout offset or the gain.

On DOY 2011304, pre-amp temperatures (recorded in the FITS header keyword 'CCDPRET') were gradually increased from 274 K to 293 K, and then decreased again. During this increase, we obtained several long exposures of 180 sec in CLEAR1, and of 480 sec using the CN filter. The length of these exposures resulted in contamination by background stars and cosmic rays. To measure the effect of the temperature change on the data while avoiding contaminating sources, we determined the median count per quadrant with rejection of extreme pixel values (we used the IDL routine 'resistant_mean.pro' from the IDL Library or the GSFC library, using a 3-sigma cut-off). We used RADREV data, i.e. images that are processed using the pipeline and from which regular electronic effects have been removed through subtraction of the count rate measured in the overclocked pixels.

The resulting median DN fluxes for both filters are shown in Figure 4. We separated the increase and decrease of the temperatures to look for possible hysteresis effects. While the measurements of individual quadrant suggest some spurious relation between temperature and flux, there is no clear relation that holds for all quadrants at the same time. The data suggest a steep increase in the median flux when the temperature was increased above 285 K, but this effect was not evidently present when the temperatures were decreased again.

The different behavior of the four quadrants might be explained by the fact that we use a single parameter 'CCDPRET' based on the current fed to the preamps to describe the temperature of all pre-amps. The thermal behavior might be better characterized by a more direct measurement of the temperatures of individual preamps. Additionally, scatter due to poor SNR of the observed background, cosmic rays, and background sky and stars could be limited by performing the same heating test with the LED on. In any case, the instrument response to these heating tests did not reproduce the effects seen during the anomaly, indicating that this phenomenon was not the cause.

2.3 Stray light

During the period of the anomaly, the spacecraft was observing Hartley 2 at an atypical attitude with respect to the solar illumination direction. The geometry was gradually changing throughout the period, with the solar elongation of the spacecraft decreasing from about 128° at DOY 2010248, to 118° at DOY 2010268. The instruments were not fully shaded by the spacecraft solar panels during this time. It seemed plausible that a stray light path to the MRI CCD could exist (if not originally, perhaps now after 6 years in flight and one close comet flyby exposing the instrument to micrometeoroid impacts). Such a path could have a narrow entrance aperture so that light can reach the CCD from behind the filter only for a very

narrow range of illumination conditions and that its intensity could gradually increase and then decrease as the illumination geometry changed.

To investigate this scenario, we sampled 10 S/C orientations that reproduced the solar elongation range during the anomaly. At each orientation, we acquired two 180 sec exposures with the CLEAR1 filter and two 480 sec exposures with the CN filter. The shutter was open during these exposures, and we again determined the median counts per pixel (sec. 2.2). The solar azimuth was fixed at -45 degrees as was the case during the CN anomaly.

The resulting median counts are shown in Figure 5. There clearly is a strong effect on the measured counts. In the clear filter, count rates peak at a solar elongation of 123 degrees with an additional signal of 0.027 DN/sec/pixel, while in the CN filter count rates are increased by 0.013 – 0.017 DN/sec/pixel. Note that this is an 8-fold increase in the CN count rate, and only a 50% increase in count rates using the CLEAR1 filter, because almost no background signal is present in regular narrowband observations. The increase is the strongest in quadrant A (top right), and inspection of the images (Figure 6) indeed shows a clear pattern on the MRI detector running from top right to bottom left on the detector. These absolute signals are very comparable to those measured during the anomalous observations (maximum median increases of 0.015 and 0.018 DN/sec/pixel in the CN and CLEAR1 filters, respectively). These results indicate that stray light can get into the MRI detector under the specific solar illumination angles that were present during the anomaly.

3. Discussion and conclusion

3.1 Test results

Each of the tests described in the previous section resulted in identifiable patterns that can be used to diagnose the anomalous MRI measurements from September 2010. Illumination by the LED light resulted in a clear pattern from left to right on the MRI CCD, and an approximately solar color. Orienting the spacecraft to reproduce the solar illumination geometry indicates the presence of an orientation-dependent light leak. Different from the LED pattern, the light leak results in a pattern that peaks in the upper right corner (Quadrant A) of the detector in observations with both the CN and CLEAR1 filters. For comparison, an image of Hartley-2 obtained during the anomaly is shown next to an image obtained during our light leak test in Figure 7. The similarity between the two images is evident and indicates that the stray light was responsible for the measured signal.

In absolute terms, the light leak enhancement during the tests was twice as strong in the CLEAR1 filter as in the CN filter (0.027 vs. 0.017 DN/s/pix), while they were roughly comparable during the approach to comet Hartley 2 (0.018 vs 0.015 DN/s/pix). However, because background levels are higher in CLEAR1, the relative effect is much stronger in observations with the CN filter (100% of the median background level for CLEAR1 vs. 800% for CN). This well explains why the observations in September 2010 were initially explained as a ‘CN-anomaly’.

We also tested the effect of increasing the temperature of the pre-amps. Beforehand, we expected that any electronically induced variation in background

signal due to changes in electronics temperatures would also affect the overclocked pixel values used in bias subtraction. The normal calibration process should correct for any electronically induced effects. Our test indicated a non-linear effect that might introduce some scatter at CCDPRET temperatures above 290 K; during the anomaly CCDPRET was not higher than 282 K. Close inspection suggested some correlation between CCDPRET and the measured signal, in particular during sudden changes in the temperature, as is demonstrated in Figure 8. Even if this correlation is real, it contributes at most 10% to the signal from the light leak during the anomaly.

3.2 Source

In order to identify the source of the light leak we show a model of the spacecraft as seen from the Sun under the geometric conditions of the spacecraft during the anomaly in Figure 9. There is clearly no direct path to the MRI. It seems most likely that Sun light is reflected off the high-gain antenna or the star trackers. Our tests suggest that light leak count rates do vary depending on what filter is used, but that light probably does not pass through the filters, i.e., light has to come in through a small hole between the filter house and the CCD.

An obvious candidate is the high gain antenna and associated structure, but the antenna was in different orientations for the approach and the anomaly test, and most of the structure other than the antenna itself does not have a direct line of sight to the MRI. Alternatively, light may be reflected off the low-gain antenna that stands up from the main bus structure right next to the instrument platform. It can be seen from Fig. 9 that during the peak anomaly brightness it was illuminated by the sun. The low gain antenna is located on a plane about the same level as the MRI and it would shine on the right side of the MRI. A pinhole that would allow light in from the low-gain would orient the light to be crossing laterally, and could reflect off the filter wheel or shutter. It is of note that the cable patch panel is located on the right hand side of the MRI (when looking from behind), and that multiple possible pinholes are available in this region.

3.3 Other occurrences

We identified about 1500 images during the prime mission that were obtained under the solar elongation angles that allowed the stray light to enter the instrument during the EPOXI mission's anomaly (elongation between 118 – 128 degrees). No images where obtained under these circumstance during the EPOCH mission. Given that we measured a maximal signal of 0.03 DN/sec/pixel using the CLEAR1 filter, and that the background count rate in this filter is also 0.03 DN/sec/pixel (Figure 5), we are unlikely to detect an effect in images acquired with an exposure time of less than 60 seconds (SNR ~ 1). This leaves a sample of 222 images, all of them obtained before the encounter with Tempel 1. Only one image in this sample was obtained using the full 1024 x 1024 frame (CLEAR1, 2005062, obsid 2100040, see Table 1), and no anomalous pattern is visible in this image. We then checked several images using the optimal elongation and longest exposure time as selection criteria (Table 1). Visual inspection of these images showed no

evidence of a light leak. One image obtained with the CN filter (DOY 2005177, obsid 6002634) has elevated count rates in quadrants A and D, but subsequent CLEAR1 filters (obsid 6002636) show no such pattern. The longest exposure (274 sec) using the CN filter was obtained on DOY 2005184 (9000240) and shows no specific pattern but was obtained with an azimuth of 15 degrees.

Of course, the light leak might have been caused by an impact during the fly-by of Tempel 1, so we also inspected the dataset post DOY 2005185. Ruling out images with exposure times less than 10 seconds leaves about 70 images obtained at the right elongation. In obsids 908002 and 909002 (both DOY 2005186) we again note elevated quadrants A and D, but as the two quadrants are up by roughly the same amount this is more likely a bias offset effect than evidence for a light leak, where we would expect a gradient from the top right to bottom left of the CCD. On DOY 2005185 and 186 several 4 second exposures were obtained using the CLEAR1 filter at an elongation of 33 degrees (e.g. obsid 9070017 and following exposures). Inspecting those images, there is a clear pattern on the right side of the detector that is reminiscent of that seen during the anomaly (Figure 10). However, given the low expected count rates (0.027 DN/sec/pixel, see Sec. 2.3), it is unlikely that a light leak pattern would be observed in such a short exposure. We conclude that the observed pattern in on DOY 2005285-286 is more likely an in internal reflection due to Tempel-1's brightness and that the dataset does not allow us to test whether the light leak was present or not during the post-encounter time frame of the prime mission.

Figures:

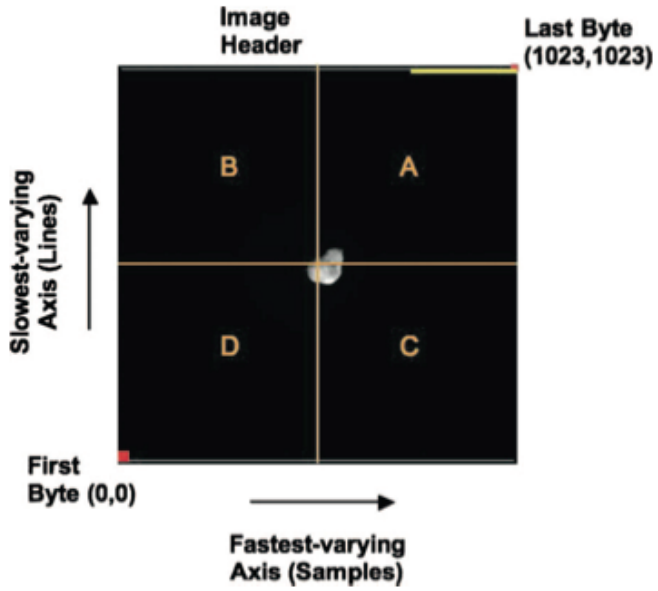

Figure 1 – *MRI Quadrant labels (A–D). We used the same labels used in Klaasen et al. 2008.*

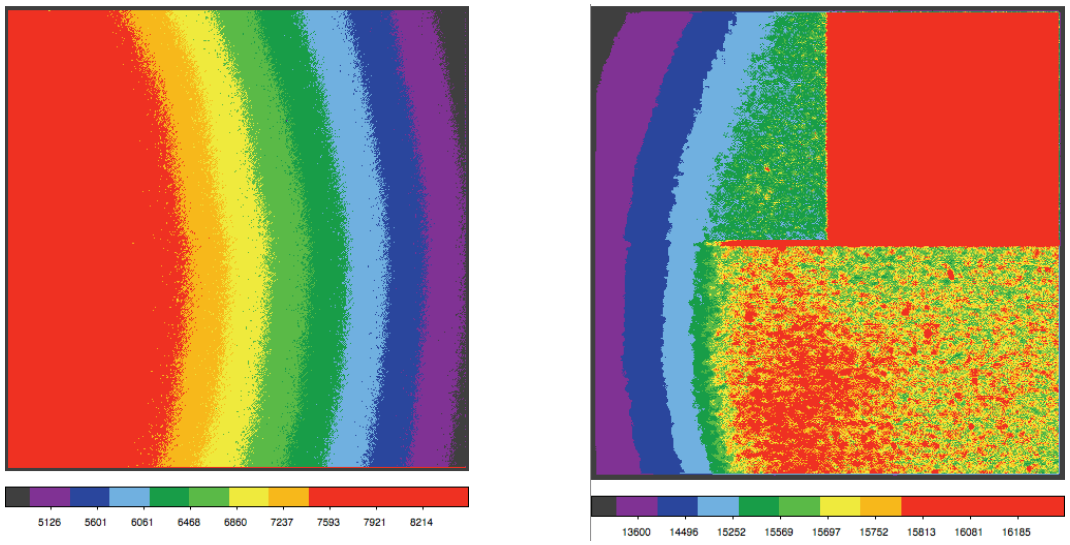

Figure 2 – *Histogram equalized MRI Clear1 (left) and HRI Clear1 (right) exposures (600 msec each), showing the patterns from LED light reflecting off the filter. The color scale is used to emphasize the curvature in the gradient.*

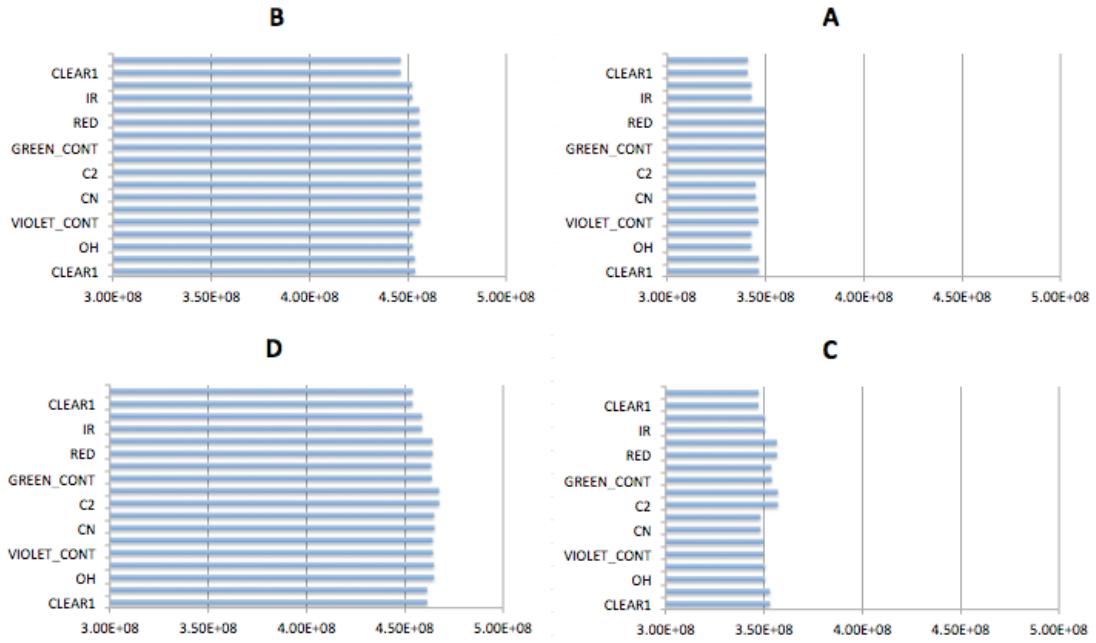

Figure 3a – *LED test: total DN per MRI quadrant for 600 msec exposures. Labels A-D indicate the different quadrants on the chip, organized according to their position (fig. 1). The filters are ordered by wavelength (longest wavelength/top to shortest wavelength/bottom).*

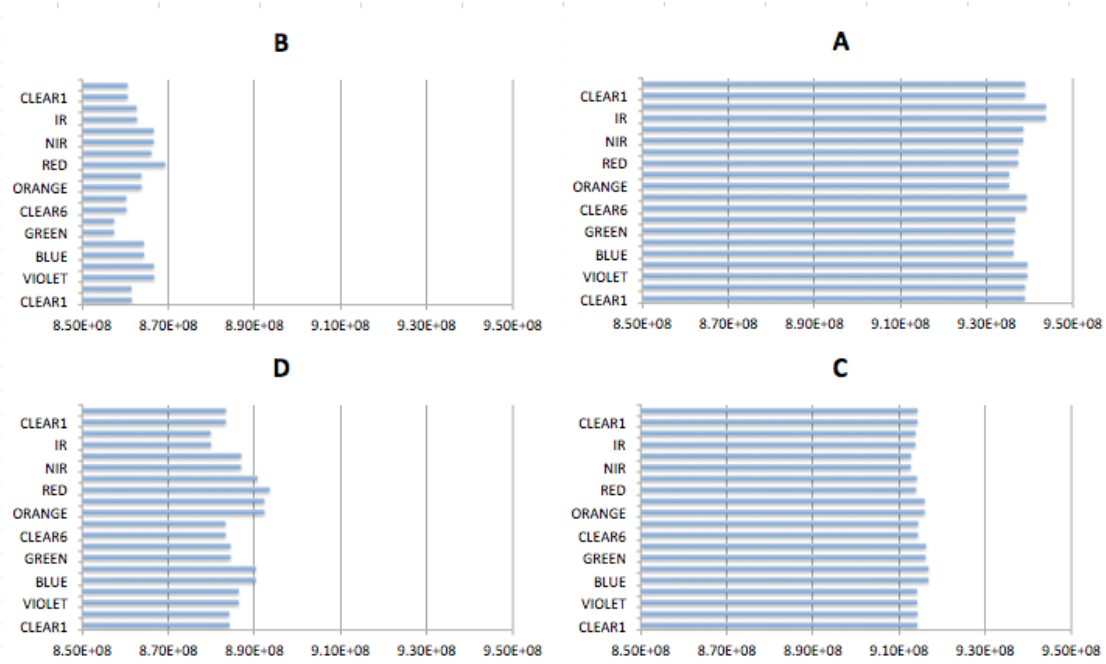

Figure 3b – *LED test: Total DN per HRI quadrant for 600 msec exposures. Labels A-D indicate the different quadrants on the chip, organized according to their position (fig. 1). The filters are ordered by wavelength (longest wavelength/top to shortest wavelength/bottom).*

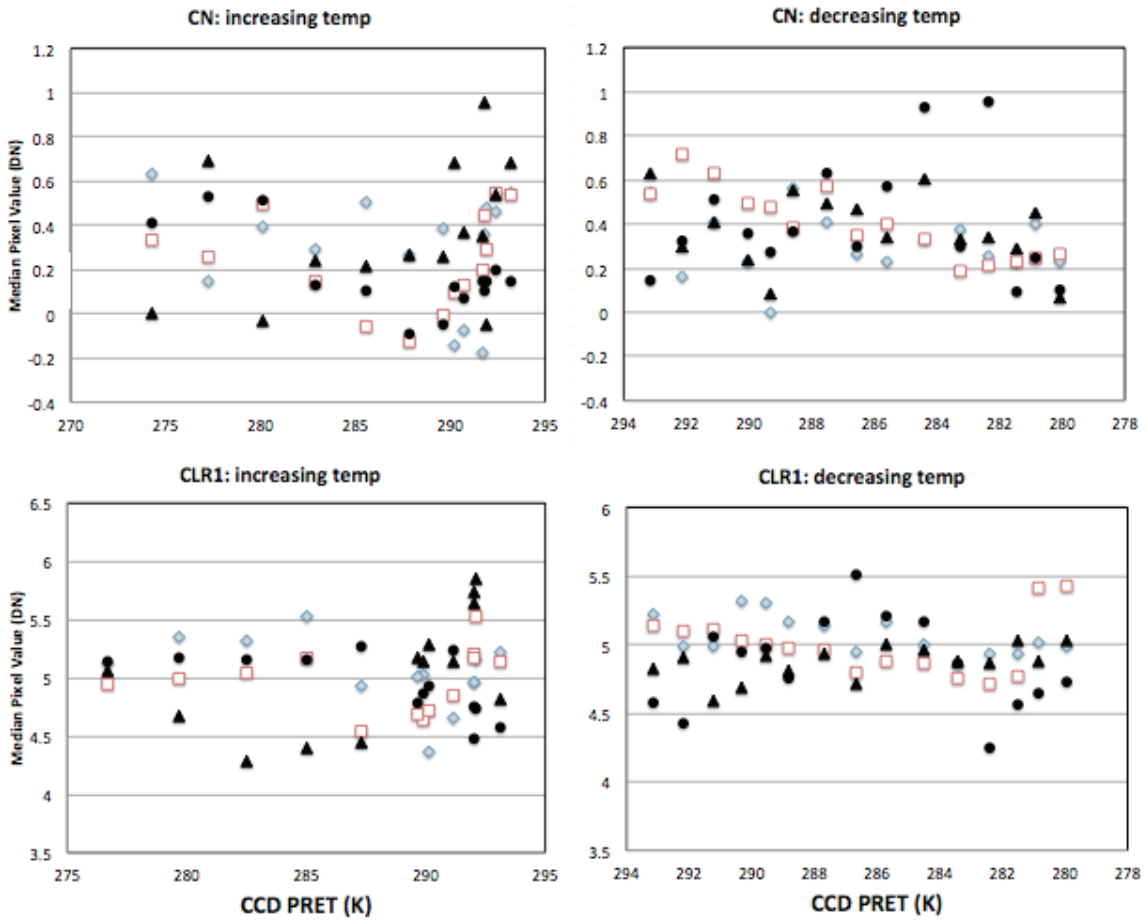

Figure 4 – *Pre-Amplifier heating test. The temperature of the pre-amps was gradually increased (left column) and then again decreased (right column). Median pixel values were determined in exposures using the CN (top row) and CLEAR1 (bottom row) filters. Quadrant A – filled black circle; B – filled black triangle; C – Red open square; D – Blue open diamond.*

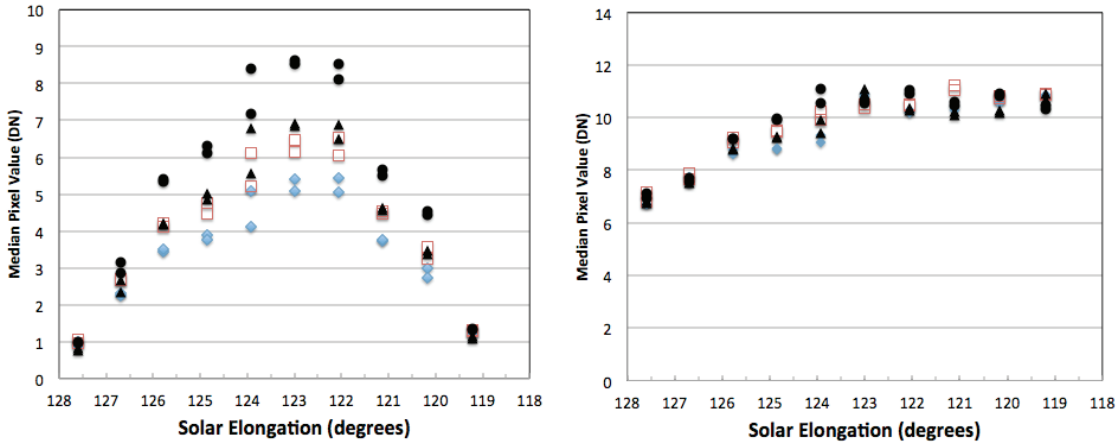

Figure 5 – *Light leak test. The solar elongation was gradually changed from 128 – 118 degrees. Median pixel values were determined in exposures using the CN (left) and CLEAR1 (right) filters. Quadrant A – filled black circle; B – filled black triangle; C – Red open square; D – Blue open diamond.*

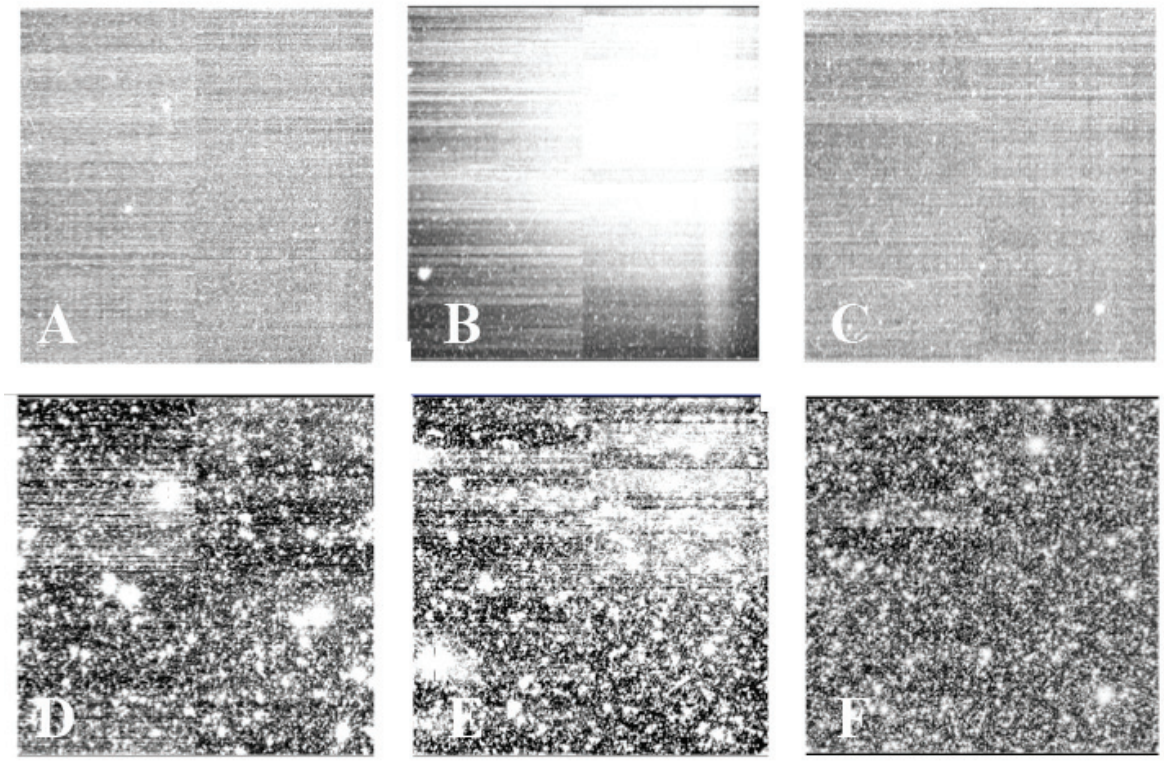

Figure 6 – *Light leak test. The spacecraft's solar elongation was gradually changed from 128 – 118 degrees and a clear pattern could be seen in the MRI images. Top row (A – C): CN filter. Bottom row (D – F): CLEAR1 filter. Both rows show the sky image at 127 deg (A,D), at 123 deg, the peak of the light leak (B,E), and at 118 deg (C,F). Images are stretched to optimally show the effects.*

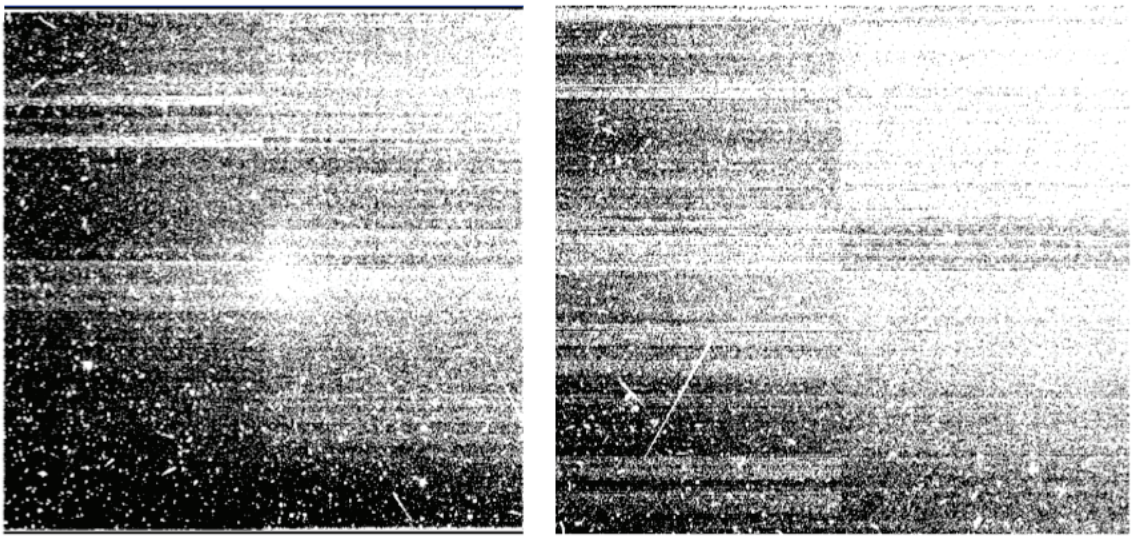

Figure 7 – *Anomaly vs. light leak test. The MRI image obtained with the CN filter during the anomaly (left) shares the same morphology as the image obtained during the light leak test (right), with enhanced scattered light in the top right corner of the detector, and a gradient from top right to lower left. The images have similar exposure times and equal scale/color bar.*

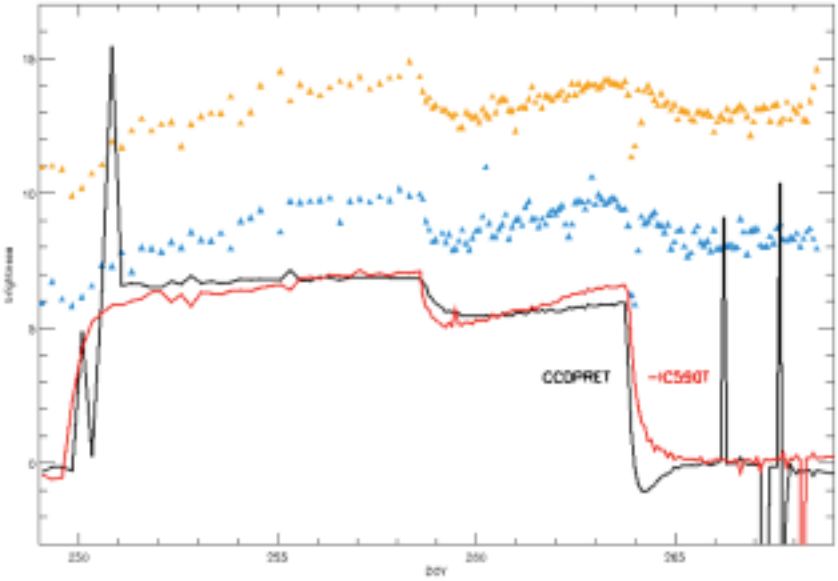

Figure 8 – *MRI count rates in quadrant A during the anomaly (blue –square close to the edge, orange, closer to the center, both offset to allow comparison) and two temperature profiles (CCDPRET; black, and IC590T, instrument controller board, inverted, red).*

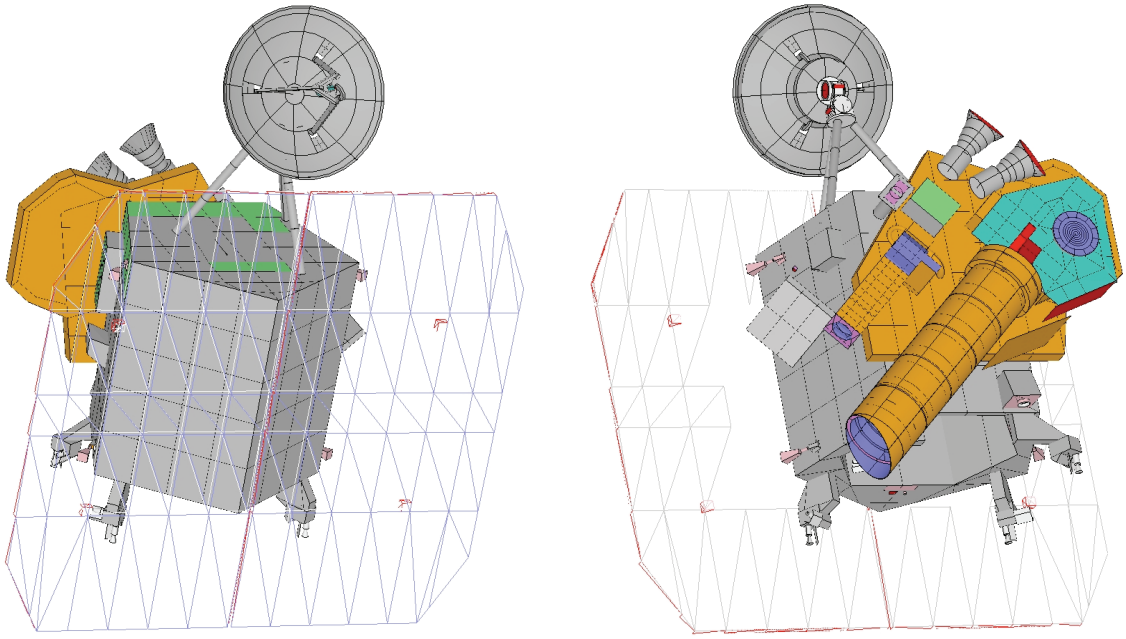

Figure 9 – *Deep Impact spacecraft as seen from the Sun (left) and anti-Sun (right). The orientation is that of the maximum anomaly, i.e. a solar elongation of 123 degrees The solar array is shown as a wire frame for illustrative purposes.*

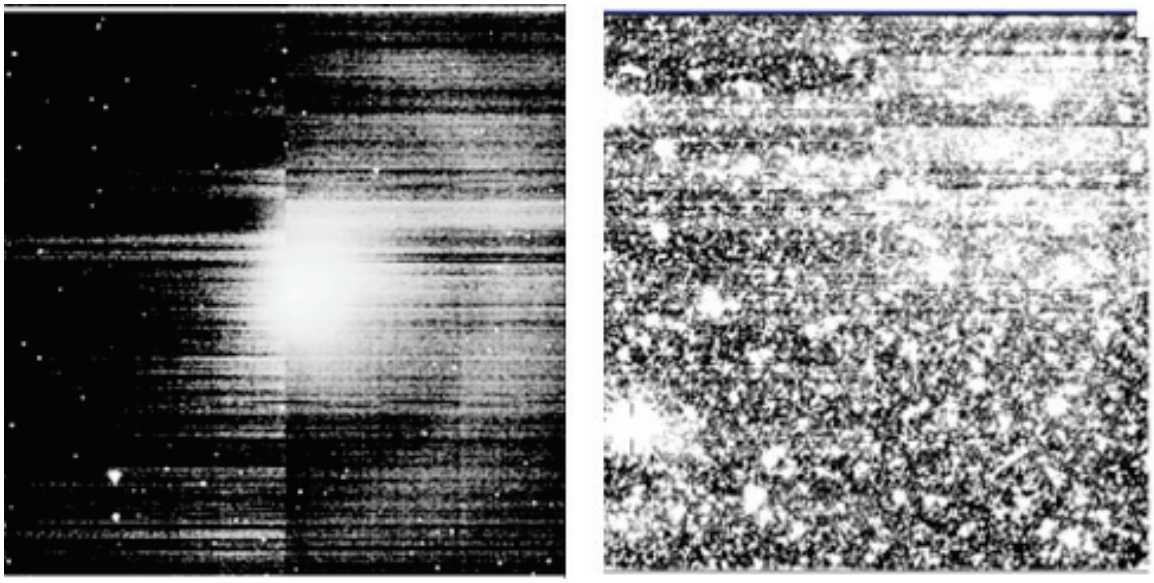

Figure 10 – *MRI CLEAR1 image of Tempel 1 (left) obtained on DOY 2005286, compared with a CLEAR1 exposure obtained during the anomaly (same as Fig. 6D).*

Table 1 – *Selected observations that were inspected for a pattern indicating the existence of a light leak during the prime mission.*

DOY	OBSID	Int. time	Filter	Framesize	Azimuth	Elon.
2005062	2100040	01:39.997	CLEAR1	1024	-44.65	117.37
2005170	6001953	00:59.997	C2	256	-45.00	123.14
2005170	6001948	00:59.997	CLEAR1	256	-45.00	123.18
2005168	6001734	00:59.997	CN	256	-45.00	124.17
2005170	6001922	00:59.997	CN	256	-45.00	123.36
2005173	6002258	00:59.997	CN	256	-45.00	121.85
2005177	6002634	00:59.997	CN	256	-45.00	120.30
2005177	6002636	00:59.997	CLEAR1	256	-45.00	120.26
2005184	9000240	04:34.997	CN	512	14.59	123.17
2005186	9080002	00:19.997	CN	1024	15.93	123.63
2005186	9090002	00:19.997	CN	1024	15.78	123.55
2005186	9070017	00:03.997	CLEAR1	1024	15.46	123.38